Avian-specific *Salmonella* transition to endemicity is accompanied by localized resistome and mobilome interaction

Chenghao Jia[1], Chenghu Huang[1,2], Haiyang Zhou[1,2], Xiao Zhou[5], Zining Wang[1,2], Abubakar Siddique[1,2], Xiamei Kang[1], Qianzhe Cao[1], Yingying Huang[1,2], Fang He [1,6], Yan Li [1,2], Min Yue [1,2,3,4#]

[1] Department of Veterinary Medicine, Zhejiang University College of Animal Sciences, Hangzhou 310058, China

[2] Hainan Institute of Zhejiang University, Sanya 572000, China

[3] School of Life Science, Hangzhou Institute for Advanced Study, University of Chinese Academy of Sciences, Hangzhou 310024, China.

[4] State Key Laboratory for Diagnosis and Treatment of Infectious Diseases, National Clinical Research Center for Infectious Diseases, National Medical Center for Infectious Diseases, The First Affiliated Hospital, College of Medicine, Zhejiang University, Hangzhou 310003, China

[5] Ningbo Academy of Agricultural Sciences, Ningbo 315040, China

[6] ZJU-Xinchang Joint Innovation Centre (TianMu Laboratory), Gaochuang Hi-Tech Park, Zhejiang, China

Email address:

CJ: 22017118@zju.edu.cn

CH: 22217106@zju.edu.cn

ZH: zhouhaiyang@zju.edu.cn

XZ: xiaozhou_2023@163.com

ZW: znwang@zju.edu.cn

AS:abubakars@zju.edu.cn

XK: 12017032@zju.edu.cn

QC: 22317128@zju.edu.cn

YH: 22317127@zju.edu.cn

FH: hefangzj@zju.edu.cn

YL: yanli3@zju.edu.cn

Corresponding author:

Min Yue. Tel: +86 0571 88982832; E-mail: myue@zju.edu.cn

Abstract:

Bacterial regional demonstration after global dissemination is an essential pathway for selecting distinct finesses. However, the evolution of the resistome during the transition to endemicity remains unaddressed. Using the most comprehensive whole-genome sequencing dataset of *Salmonella enterica* serovar Gallinarum (*S*. Gallinarum) collected from 15 countries, including 45 newly recovered samples from two related local regions, we established the relationship among avian-specific pathogen genetic profiles and localization patterns. Initially, we revealed the international transmission and evolutionary history of *S*. Gallinarum to recent endemicity through phylogenetic analysis conducted using a spatiotemporal Bayesian framework. Our findings indicate that the independent acquisition of the resistome via the mobilome, primarily through plasmids and transposons shapes a unique antimicrobial resistance profile among different lineages. Notably, the mobilome-resistome combination among distinct lineages exhibits a geographical-specific manner, further supporting a localized endemic mobilome-driven process. Collectively, this study elucidates resistome adaptation in the endemic transition of an avian-specific pathogen, likely driven by the localized farming style, and provides valuable insights for targeted interventions.

Keywords:

Salmonella; Mobilome; Resistome; Whole genome sequencing; Horizontal gene transfer

Introduction

The acquisition of antimicrobial resistance (AMR) by pathogens is well-established as one of the most severe threats of the 21st century (1–3). It is estimated that over 10 million people could die per year due to AMR by 2050 (4). Antimicrobial resistance genes (ARGs), collectively known as the resistome, play a pivotal role in AMR development, progression, and amplification (5). Pathogens typically acquire resistome through mobilomes, like plasmids, via horizontal gene transfer (HGT) (6, 7). From an evolutionary perspective, the dynamic change in the resistome is crucial for enhancing pathogen fitness and enabling it to colonize new ecological niches (8). Key factors contributing to resistome alterations include disease burden, human activities, climate change, and geographical selection forces (9–13). Understanding the evolutionary trajectory of the AMR and related reservoirs is necessary, as disease management strategies will differ substantially (14). However, knowledge regarding the overall profile of pathogen regional adaptation related to the stepwise dynamics of the resistome remains limited.

Before recent advancements in whole-genome sequencing (WGS) technology, little was understood about resistome diversity that affects pathogen endemicity (15). Traditional typing methods generally exhibit low resolution, making monitoring and quantitatively comparing horizontal ARG transfer events challenging. The scarcity of appropriate models also poses a limitation. *Salmonella*, a widespread foodborne and zoonotic pathogen with distinct geographical characteristics, has more than 90% of its serovars typically classified as geo-serotypes (16, 17). Among the thousands of geo-serotypes, *Salmonella enterica* serovar Gallinarum (*S*. Gallinarum) is an avian-specific pathogen that causes severe mortality, with particularly detrimental effects on the poultry industry in low- and middle-income countries

(18–20). As once a globally prevalent pathogen in the 20th century, *S*. Gallinarum was listed by the World Organization for Animal Health (WOAH) and gradually became an endemic pathogen with sporadic outbreaks following the implementation of eradication programs in most high-income countries, making it a perfect model for study (21, 22).

Nowadays, antimicrobial therapy remains a priority choice against *S.* Gallinarum infections (23). The overuse or misuse of antimicrobials has led to increased epidemiological escalation of *S.* Gallinarum, with a regionally higher risk of AMR, especially for sulfonamides, penicillin, and tetracyclines (24, 25). To fill the gaps in understanding the evolution of *S.* Gallinarum under regional-associated AMR pressures and its adaptation to endemicity, we collected the most comprehensive set *S*. Gallinarum isolates, consisting of 580 genomes, spanning the period from 1966 to 2023. Using such a unique WGS dataset, we investigated: 1) the population structure and potential geographical transmission history of *S.* Gallinarum at a single base level; 2) the dynamic resistome and mobilome changes that are associated with *S.* Gallinarum transition to an endemic variant; and 3) horizontal resistome transfer frequency and pattern between distinct regions.

Results

Global distribution of *S.* Gallinarum links with distinct sublineages

To understand the global geographic distribution and genetic relationships of *S*. Gallinarum, we assembled the most comprehensive *S.* Gallinarum WGS dataset (n=580, Supplementary Table 1 and 2), comprising 535 publicly available genomes and 45 newly sequenced genomes (26)***.*** The core-genome single nucleotide polymorphism sites (cgSNPs) were obtained by using the fully sequenced genome of *S.* Gallinarum R51 as a reference. Through hierarchical

Bayesian analysis of cgSNPs, it was confirmed that *S.* Gallinarum divides into three biovars: *S*. Gallinarum biovar Pullorum (bvSP) (n=528/580, 91.03%), *S*. Gallinarum biovar Gallinarum (bvSG) (n=50/580, 8.6%), and *S*. Gallinarum biovar Duisburg (bvSD) (n=2/580, 0.34%). An association was identified between the biovar type of *S.* Gallinarum and its global geographic distribution. Most bvSP isolates were from Asia (436/528), with fewer occurrences in Europe (54/528), South America (12/528), and North America (5/528). In bvSG, South America (18/50, 36%) is the primary source of isolates, followed by North America (9/50, 18%), Europe (9/50, 18%), Africa (7/50, 14%), and Asia (3/50, 6%) (S1 Fig).

From a lineage perspective, bvSP can be further classified into five lineages: L1 (10/528), L2a (45/528), L2b (163/528), L3b (169/528), and L3c (141/528). Importantly, L3a, previously considered distinct, has been revealed as a sub-lineage of L3c. The predominant lineage types vary across different continents. Regarding predominant bvSP sources, Asia stands out, with L3c, L3b, and L2b being the main lineage types. On the other hand, L3b and L2a are more widespread in Europe and America, respectively (Fig 1a). For the bvSP strains from Asia included in our dataset, we found that all originated from China. To further investigate the distribution of bvSP across different regions in China, we categorized them into three distinct regions: southern, eastern, and northern (Supplementary Table 3). Our findings indicate significant variations in bvSP across various regions from geo-temporal aspects. Prevalence was highest in the eastern region (233/436), with lower incidences in the northern (137/436) and southern regions (65/436). Interestingly, the predominant bvSP lineage type also varied. In eastern and southern China, L2b and L3c exhibited as the predominant lineage types, while in northern China, L3b and L3c held nearly equivalent positions (Fig 1b**)**.

An analysis of the temporal prevalence of bvSP in China revealed a gradual replacement pattern of the lineages. Before the 2000s, the predominant lineage type was L3b. Then, from the 2000s to the 2010s, L3b and L1 were continually replaced by L3c, with L2b becoming the predominant lineage after the 2010s (Fig 1c). However, the replacement pattern varied among different regions. Specifically, the same pattern was observed in eastern China, but for northern and southern China, only replacements from L3b to L2b and L1 to L3c were observed (S2 Fig). These findings might indicate accelerated localized adaptation of bvSP.

Genomics portrait bvSP historic transmission

Considering the historical pandemic status of bvSP, we then investigated its global geographic transmission routes to understand its evolution into an endemic pathogen. L2b and L3b were identified as the dominant global lineages due to their antimicrobial resistance risks, and potential intercontinental transmission events. Other lineages were also analyzed using a Bayesian model with a relaxed molecular clock to infer their historical evolution (S3-S5 Figs). The temporal structure was verified (S6 Fig). Our findings show that the origin of L3b in China can be traced back to as early as 1683 (95% CI: 1608 to 1839). In contrast, the earliest possible origin of L2b in China dates back to 1880 (95% CI: 1838 to 1902) (Fig 2). Then, we specifically estimated the time points for the first intercontinental transmission events for the two major lineages. Our results indicate that L2b, likely underwent two major intercontinental transmission events. The first occurred around 1893 (95% CI: 1870 to 1918), with transmission from China to South America. The second major transmission event occurred in 1923 (95% CI: 1907 to 1940), involving the spread from South America to Europe. In contrast, the transmission pattern

of L3b, an *S*. Gallinarum lineage originating in China, appears relatively more straightforward. It underwent only one intercontinental transmission event, from China to Europe, likely around 1790 (95% CI: 1661 to 1890) (S7 Fig).

Endemic isolates further support localized dissemination by bvSP

To investigate the dissemination pattern of bvSP, we obtained forty-five newly isolated bvSP from 734 samples (6.1% overall isolation rate) collected from diseased chickens at two farms in Yueqing and Taishun, Zhejiang Province. Those bvSP can be classified into two dominant sequence types (STs): ST3717 and ST92. Isolates from Yueqing were all identified as ST3717, while most Taishun isolates were characterized as ST92. Only the E404 isolate was identified as ST2151 (Fig 3a). Of note, a lineage-preferential association was also observed, with bvSP isolated from Taishun belonging to L3b and those from Yueqing belonging to L2b. To further understand the genetic relationship among isolates in the two regions, we calculated cgSNPs distances between isolates. Isolates with cgSNP distances less than two were determined as the threshold to be involved in the same transmission event. Interestingly, genetic clustering revealed that isolates from the same farm exhibited a significantly close genetic correlation (Fig 3b). No historical transmission events of bvSP were found between Taishun and Yueqing.

Other genetic characteristics also exhibited a similar pattern. The ARG and plasmid profile disclosed that *IncFII(S)* and *ColpVC* plasmids exhibited the highest carriage percentages (100%) among the 45 bvSP isolates. The *IncX1* plasmid was exclusively identified in the E404 isolate. Furthermore, E404 harboured two distinctive resistance genes, $bla_{\text{TEM-1B}}$ and *sul2*, in contrast to the absence of ARGs in the remaining bvSP isolates. We also estimated the invasiveness index to assess the invasiveness of isolated bvSP and showed

that bvSP from the same farm had comparable invasive abilities. However, isolates from Taishun demonstrated a higher invasive ability than those from Yueqing (Fig 3c, Supplementary Table 4).

Furthermore, we simulated potential transmission events between the bvSP strains isolated from Zhejiang Province (n=95) and those from China with available provincial information (n=435) using two SNPs as the threshold. As a result, the transmission events showed a strong geographic-preferential distribution. We identified a total of 53 potential transmission events, all of which occurred exclusively within Zhejiang Province. No inter-provincial transmission events were detected, supporting the statement that bvSP in China is a highly localized pathogen (S8 Fig, Supplementary Table 5).

Mobilome and resistome distinct lineage-preferential association in a regional manner

The mobilome drives partitions of the resistome and plays a pivotal role in shaping the ecological niches and local adaptation of bacteria. Therefore, a quantitative evaluation of the resistome and mobilome is necessary to enhance the understanding of the localized distribution of bvSP. For *S.* Gallinarum, a total of 13 classes of ARGs, which can be further classified into six categories, were identified. The results revealed that bvSP exhibited a significantly greater resistome than bvSG and bvSD (Fig 4a). Among them, *sul2* (196/528, 37.1%) has the highest prevalence, followed by $bla_{\text{TEM-1B}}$ (183/528, 34.7%) and *tet(A)* (104/528, 19.7%). Moreover, the resistome also demonstrated a lineage-preferential association. We observed that L3b is more inclined to carry $bla_{\text{TEM-1B}}$ and *sul2* than other lineages, whereas *tet*(A) exclusively exists within L3 (Supplementary Table 6). The diversity of resistome carried by L3 may elevate the risk of multi-drug resistance (MDR). Notably, AMR risks vary among

different regions of China, with the highest risk observed in southern China, followed by the northern and eastern regions. Interestingly, *tet(A)*, *bla*$_{\text{TEM-1B}}$, and *sul2* were predominant resistome types prevalent across all regions of China. Meanwhile, *aadA5* was typically more commonly found in southern China (Fig 4b and c).

Four categories of the mobilome—prophage, plasmid, transposon, and integron—were characterized, revealing strong lineage-specific patterns (S9a Fig, Supplementary Table 7). In silico analyses revealed prophages emerge as the most diverse mobilome type, with *Entero_mEp237*, *Escher_500465_1, and Klebsi_4LV2017* being more likely associated with L1, L2a, and L2b, respectively, while the carrier percentage of *Escher_pro483* is significantly higher among L3c. Interestingly, *Salmon_SJ46, Gifsy_2*, *Escher_500465_2,* and *Shigel_SfIV* were consistently observed across all bvSP lineages and were found to be duplicated on the chromosome. For plasmids, *IncFII(S)* was predominantly carried across all bvSP lineages (520/528, 98.5%) (S9b Fig). Notably, *ColpVC* had the lowest carriage percentage among L1 (2/10, 20%), whereas *IncX1* was explicitly associated with L3c (140/141, 99.3%).

The diversity of transposons and integrons is comparatively lower in bvSP. Specifically, we identified seven types of transposons and four types of integrons. Transposons were found to be more abundant, comprising a total of 255 in 528 bvSP. Among them, *Tn801* (185/528, 35%) had the highest carriage rate, followed by *Tn1721* (48/528, 9.1%). Interestingly, L3c is more likely to carry *Tn801* and *Tn1721* transposons than other lineages. In contrast, a total of 42 integrons were identified among the 528 bvSP, all of which belong to class I: *In498* (n=22), *In1440* (n=14), *In473* (n=4), and *In282* (n=2). The integrons also exhibited a lineage-preferential distribution, predominantly carried by L3b.

From a geographic distribution perspective, bvSP from northern and southern China carried the most extensive mobilome, followed by those from eastern China. Interestingly, bvSP isolated from northern China typically have more diverse mobilome types (S10 Fig).

Plasmid and transposon guide resistome geo-temporal dissemination

Variations in regional antimicrobial use may result in uneven pressure for selecting AMR. The mobilome is considered the primary reservoir for spreading resistome, and a consistent trend between the resistome and the mobilome has been observed across different lineages, from L1-L3c. We observed an overall gradual rise in the resistome quantity carried by bvSP across various lineages, correlating with the total mobilome content (S11 Fig). Furthermore, we investigated the interplay between particular mobile elements and resistome types in bvSP.

In bvSP, the predominant resistome is mainly associated with certain types of mobilome (Fig 5a). Specifically, regarding $bla_{\mathrm{TEM_1B}}$, *tet(A)*, and *sul1*, which are highly prevalent among bvSP, we found most $bla_{\mathrm{TEM_1B}}$ were carried by the transposon *Tn801* and *Tn1721*, the plasmid *IncX1*, and the prophage SJ46. Additionally, *tet(A)* was primarily associated with the transposon *Tn1721* and the plasmid IncX1. Integrons also facilitated the dissemination of the resistome. For instance, *In498* and *In1440* facilitate the dissemination of *sul1*, leading to quinolone resistance. Our results indicate that plasmids and transposons are the predominant reservoirs for the resistome in bvSP, with prophages and integrons following closely behind (Fig 5b). Interestingly, we observed that the primary reservoir for the resistome shows regional variations. In the southern and northern regions of China, the primary reservoirs for $bla_{\mathrm{TEM_1B}}$ are *Tn801*, *Tn1721*, *IncX1*, and prophage SJ46. However, *Tn1721* was less frequently

found in bvSP, which carries *bla*$_{TEM-1B}$ from the eastern region. Similarly, the reservoir for *tet(A)* exhibits greater diversity in the east region but less diversity in the southern region (Fig 5c-e).

Horizontal transfer of resistome occurs widely in localized bvSP

Horizontal transfer of the resistome facilitates the acquisition of AMR among bacteria, which may record the distinct acquisition event in the bacterial genome. To compare these events in a geographic manner, we further investigated the HGT frequency of each ARG carried by bvSP isolated from China and explored the HGT frequency of resistome between three defined regions. Potentially horizontally transferred ARGs were defined as those with perfect identity (100% identity and 100% coverage) and were located on MGEs across different strains (Fig. 6a). We first categorized a total of 621 ARGs carried by 436 bvSP isolates collected in China and found that 415 ARGs were located on MGEs (Supplementary Table 8). After excluding the ARGs not associated with MGEs, our findings reveal that horizontal gene transfer of ARGs is widespread among Chinese bvSP isolates, with an overall transfer rate of 92%. Specifically, 50% of the ARGs exhibited an HGT frequency of 100%. Using the HGTphyloDetect pipeline, we verified the HGT transmission potential for each ARG sequence. The results demonstrated that ARGs with an HGT frequency greater than zero (*bla*$_{TEM-1B}$, *sul1*, *dfrA17*, *aadA5*, *sul2*, *aph(3'')-Ib*, *tet(A)*, *aph(6)-Id*) all had Alien Index scores exceeding 45 and out_perc values greater than 90, indicating that these ARGs may have undergone extensive horizontal transfer events (Fig. 6b, Supplementary Table 9). It is noteworthy that certain resistance genes, such as *tet(A)*, *aph(3")-Ib*, and *aph(6)-Id*, appear to be less susceptible to horizontal transfer.

However, different regions generally exhibited a considerable difference in resistome HGT frequency. For specifical ARG type, we found *tet(A)* is more prone to horizontal transfer in the southern region, and this proportion was considerably lower in the eastern region. Interestingly, certain ARGs, such as *aph(6)-Id*, undergo horizontal transfer only within the eastern and northern regions of China (Fig. 6c). Notably, as a localized transmission pathogen, resistome carried by bvSP exhibited a dynamic potential among inter-regional and local demographic transmission, especially from northern region to southern region (HGT frequency=93%) (Fig. 6d, Supplementary Table 10).

Discussion

Over the past decades, the emergence of AMR has garnered significant attention from both public health agencies and the poultry industry (27). Region-associated pressures shaped the dissemination patterns of bacterial pathogens, transitioning from pandemic to endemic, and led to dynamic changes in the resistome. Here, utilizing *S.* Gallinarum as a prototype for an endemic pathogen that once spread globally, and assembling the most comprehensive *S.* Gallinarum WGS database, we have discovered that region-associated pressures can influence the AMR risks of *S.* Gallinarum within lineage- and region-specific patterns. These pressures might also influence lineage-distinct evolutionary structures and transmission histories of *S.* Gallinarum.

The biovar types of *S*. Gallinarum have been well-defined as bvSP, bvSG, and bvSD historically (28). Among these, bvSP can be further subdivided into five lineages (L1, L2a, L2b, L3b, and L3c) using hierarchical Bayesian analysis.

Different sublineages exhibited preferential geographic distribution, with L2b and L3b of bvSP being predominant global lineage types with a high risk of AMR. The historical geographical transmission was verified using a spatiotemporal Bayesian framework. The result shows that L3b was initially spread from China to Europe in the 18th-19th century, which may be associated with the European hen fever event in the mid-19th century (29). L2b, on the other hand, appears to have spread to Europe via South America, potentially contributing to the prevalence of bvSP in the United States. Considering the economic losses caused by bvSP, the United States, Europe, and other industrialized countries implemented eradication programs in the mid-19th century, thus eliminating the risk of pullorum disease. Implementing similar measures is challenging due to China's vast geographical area and various economic factors, resulting in bvSP becoming an endemic pathogen, mainly in China.

Additionally, forty-five new bvSP isolates were obtained from two different locations (Taishun and Yueqing, Zhejiang Province). The cgSNP distances (<2 SNPs) revealed potential transmission events occurring exclusively among isolates from the same location. Traceback analysis using isolates from Zhejiang Province and other Chinese isolates with available provincial information further supports that bvSP in China is a highly localized pathogen. Moreover, the invasiveness index of bvSP from Taishun and Yueqing suggests that different lineages of *S*. Gallinarum recovered from distinct regions may exhibit biological differences. Previous studies have shown that strains with higher invasiveness indexes tend to be more virulent in hosts (30, 31), potentially causing neurological or arthritic symptoms in *S*. Gallinarum infections. Furthermore, strains with varying invasiveness indexes have been

confirmed to differ in their biofilm formation abilities and metabolic capacities for carbon compounds (32).

Humanity appeared powerless against epidemics until the advent of antimicrobials, which are still the primary agents used to combat *S.* Gallinarum infection (33, 34). As a manifestation of localization-related forces, the emergence of AMR allows pathogens to acquire additional fitness benefits (35). Our findings further indicate that the mobilome facilitates the acquisition of AMR among bvSP, mainly through plasmids and transposons, such as *IncX1*, *IncQ1*, and *IncN* type plasmids, as well as *Tn801*, *Tn6205*, and *Tn721* type transposons. A survey conducted in China between 1962 and 2010 documented the association of class 1 integrons with AMR among bvSP (36). Our study further demonstrates that *In498*, *In1440*, *In473*, and *In282*, all belonging to class 1 integrons, play a significant role in carrying ARGs associated with sulfonamides, and trimethoprim. However, compared to other *Salmonella* serovars (37–39), the level of resistome in bvSP remains lower.

Considering lineage prospects, recently emerged lineages present a higher risk of AMR, with a lineage-specific distribution of resistome. In L2b and L3c, the most prevalent groups of ARGs include $bla_{\text{TEM-1b}}$ and *sul2*. L3c, which exhibits the highest resistome richness with *sul1*, *tet(A)*, *aadA5*, and *dfrA17*, has a higher likelihood of MDR. However, the transmission routes of resistome showed a high degree of consistency across continents. Globally, a small proportion of resistome carriers belonging to L2b and L3b were observed in the Americas and Europe, while isolates from Asia exhibited a notable rise in resistome carriage. Therefore, we speculate that the mobilome in bvSP may have been acquired locally in Asia, possibly due to increased antimicrobial usage and an intensive industrialized poultry farming pattern within the

regional poultry industry (40). The L3c, being a local Asian lineage and more prone to acquiring additional resistome locally, provided further support.

In China, the endemic region of Asia, an unexpected rising trend has been observed from the 1970s to the 2020s. However, the risk of AMR varies among distinct regions (41–44). Overall, the average number of ARGs carried by bvSP isolated from eastern China was the lowest, while it was higher among bvSP isolated from northern and southern China. This variation may be influenced by differences in the economy, climate, or farming practices among different regions. Interestingly, the widespread horizontal transfer of the resistome across regions indicates that the resistome has a different mode of transmission compared to its pathogenic bacteria. Specifically, as a localized pathogen, our results show a low frequency of cross-regional transmission of bvSP, but up to 90% of ARGs are transmitted cross-regionally. This risk has not been previously observed in *S.* Gallinarum, suggesting that potential intermediate hosts may play a key role.

In summary, the findings of this study highlight that *S*. Gallinarum remains a significant concern in developing countries, particularly in China. Compared to other regions, *S*. Gallinarum in China poses a notably higher risk of AMR, necessitating the development of additional therapies, i.e. vaccine, probiotics, bacteriophage therapy in response to the government's policy aimed at reducing antimicrobial use (45, 46). Furthermore, given the dynamic nature of *S*. Gallinarum risks across different regions, it is crucial to prioritize continuous monitoring in key areas, particularly in China's southern regions where extensive poultry farming is located. Lastly, from a One-Health perspective, controlling AMR in *S*. Gallinarum should not solely focus on local farming environments, with improved overall welfare on poultry and farming style. The

breeding pyramid of industrialized poultry production should be targeted at the top, with enhanced and accurate detection techniques (47). More importantly, comprehensive efforts should be made to reduce antimicrobial usage overall and mitigate potential AMR transmission from environmental sources or other hosts (48–50).

However, the current study has some limitations. Firstly, despite assembling the most comprehensive WGS database for *S.* Gallinarum from public and laboratory sources, there are still biases in the examined collection. The majority (438/580) of *S.* Gallinarum samples were collected from China, possibly since the WGS is a technology that only became widely available in the 21st century. This makes it impractical to sequence it on a large scale in the 20th century, when *S.* Gallinarum caused a global pandemic. So, we suspect that human intervention in the development of this epidemic is the main driving force behind the fact that most of the strains in the data set originated in China. In our future work, we aim to actively gather more data to minimize potential biases within our dataset, thereby improving the robustness and generalizability of our findings. Secondly, in silico analysis relies heavily on sophisticated, continuously updated databases. Although we utilized the most up-to-date databases, the exact prevalence of mobilome genetic elements (MGEs) and ARGs may be underestimated. Nevertheless, by using the most extensive global WGS data from *S.* Gallinarum, we elucidate a dynamic resistome evolution framework in a single bacterial pathogen from pandemic to endemic, which is hallmarked by a gradual increase in antimicrobial resistance risks and a stepwise resistome adaptation. The insights gained in this study will be helpful in further prevention and surveillance of the AMR risks of localized pathogens.

Material and Methods

Ethics statements

The protocols used for animal studies were approved by the Committee of the Laboratory Animal Center of Zhejiang University (ZJU20190094; ZJU20220295).

Bacterial isolates

All 734 samples of dead chicken embryos aged 19 to 20 days were collected from Taishun and Yueqing in Zhejiang Province, China. After a thorough autopsy, the liver, intestines, and spleen were extracted and added separately into 2 mL centrifuge tubes containing 1 mL PBS. The organs were then homogenized by grinding. In the initial enrichment phase, we utilized Buffered Peptone Water (BPW, Haibo Biotechnology Co, Qingdao, China), employing a 1:9 dilution ratio (sample in PBS: BPW). Subsequently, the composite was incubated at 37°C for 16-18 hours in a rotary incubator set to 180 rpm. For selective enrichment, Tetrathionate Broth Base (TTB, Land Bridge Biotechnology Co, Beijing, China), fortified with iodine solution and brilliant green solution (both from Land Bridge Biotechnology Co, Beijing, China), was employed at a ratio of 1:10 (sample in BPW: TTB). The mixture was subjected to incubation at 42°C for a duration ranging between 22 and 26 hours within a rotary incubator set at 180 rpm. Isolated *Salmonella* colonies from positive samples were obtained by sub-culturing selectively enriched samples on Xylose Lysine Deoxycholate (XLD, Land Bridge Technology Co, Beijing, China) agar, followed by an 18–22-hour incubation at 37°C. Typical and pure colonies

were selected after sub-culturing on XLD agar and transferred into Luria-Bertani (LB) broth. Finally, the transferred bacterial culture underwent an additional incubation for 18-22 hours at 37°C in a rotary incubator operating at 180 rpm.

DNA extraction and genomic assembly

The DNA of forty-five isolates was extracted using the Vazyme Fastpure® Bacteria DNA Isolation Mini Kit (Vazyme Biotech Co., Ltd.), which was then quantified using the NanoDrop1000 system (Thermo Fisher Scientific, USA). Subsequently, DNA libraries were constructed and subjected to sequencing using the Illumina Novaseq 6000 platform (Beijing Novogene Co., Ltd). Assembly of genome sequences was performed by SPAdes (51) v3.12.0 with default parameters.

Global dataset assembly

To provide global context, we expanded the dataset by including 540 additional WGS genome data, consisting of bvSP (n=483), bvSG (n=50), bvSD (n=2), and *Salmonella enterica* serovar Enteritidis (n=5). The inclusion of five strains of *Salmonella enterica* serovar Enteritidis enhanced evolutionary analyses. Notably, in this collection of 540 genomic data from public databases, 325 sequences were previously preserved in our laboratory.

All WGS data passed strict quality control according to criteria set by the European Reference Laboratory (52). Genomic data exceeding 500 contigs and having an N50 of less than 30,000 were excluded. Lastly, the bacterial species associated with each genomic data set was confirmed by utilizing KmerFinder (53) v3.2. Finally, the assembled database includes a total of 585 high-quality sequences.

Genotyping and phylogenetic analyses

Snippy v.4.4.5 was used to identify cgSNPs, with the complete genome of R51 used as a reference. The optimal model (TVM+F) was determined and employed to construct the maximum-likelihood phylogenetic tree using IQ-TREE v.1.6 (54). The final phylogenetic tree was annotated and visualized using iTOL v.6.0 (55).

The global assembly of *S.* Gallinarum underwent a population structure analysis using the RhierBAPS v1.1.4 (56), based on the Hierarchical Bayesian clustering (BHC) algorithm and employing cgSNPs as input. The calculation of population structure utilized R package v.4.3.1, supplemented by the R packages "phytools" v.2.0.3, "ape" v.5.7.1, and "rhierbaps" v.1.1.4. Default parameters were employed for all population structure analysis.

Temporal and phylogeographical analysis

To examine the emergence and geographical transfers, we first utilized Gubbins v.2.3 (57) to eliminate the recombination regions for each lineags (S12 Fig**).** Then, TreeTime (58) was used to assess the temporal structure. This was accomplished through regression analysis of the root-to-tip branch distances within the maximum likelihood tree, considering the sampling date as a variable. Then, the strains within the dataset underwent phylogeographical reconstruction via Bayesian Evolutionary Analysis of Sampled Trees (BEAST) (59) v.2.5. To determine the optimal model for running BEAST, we tested a total of six combinations in the initial phase of our study. These combinations included the strict clock, relaxed lognormal clock, and three population models (Bayesian SkyGrid, Bayesian Skyline, and Constant Size). Before conducting the full BEAST analysis, we evaluated each combination using a Markov Chain

Monte Carlo (MCMC) analysis with a total chain length of 100 million and sampling every 10,000 iterations. We then summarized the results using NSLogAnalyser and determined the optimal model based on the marginal likelihood value for each combination. The results indicated that the model incorporating the Bayesian Skyline, and the relaxed lognormal clock yielded the highest marginal likelihood value in our sample. Consequently, we proceeded to perform a time-calibrated Bayesian phylogenetic inference analysis for each lineage. The following settings were configured: the "GTR" substitution model, “4 gamma categories”, the "Relaxed Clock Log Normal" model, the "Coalescent Bayesian Skyline" tree prior. Convergence was assessed using Tracer, with all parameter effective sampling sizes (ESS) exceeding 200. Maximum clade credibility trees were generated using TreeAnnotator v.2.6.7. Finally, key divergence time points (with 95% credible intervals) were estimated and the phylogenetic tree was visualized using Figtree v.1.4.3.

SNP distance-based *S*. Gallinarum geographical tracing

To understand potential transmission events, we calculated the cgSNPs distance between distinct bacterial strains employing the SNP-dists. We estimated the overall evolutionary rate of the *S*. Gallinarum using BEAST. We applied the methodology described previously (60). The numbers of SNPs per year were determined by multiplying the evolutionary rates estimated with BEAST by the number of core SNP sites identified in the alignments. We hypothesize that a slower evolutionary rate in bacteria typically requires a lower SNP threshold when tracing transmission events using SNP distance analysis. Previous research found an average evolutionary rate of 1.97 SNPs per year (95% HPD, 0.48 to 4.61) across 22 different *Salmonella* serotypes. Our updated BEAST estimation for the evolutionary rate of *S*. Gallinarum suggests it is approximately 0.74 SNPs per year (95% HPD, 0.42 to 1.06). Based on

these findings, as well as our previous experience with similar studies (61), we set a threshold of 2 SNPs (approximately representing less two years of evolution). Additionally, the geographic location was considered to enhance the precision of speculation regarding potential transmission sites and transmission direction.

MGE detecting

Four types of MGEs were detected: plasmids, transposons, integrons, and prophages. Plasmids were detected using Abricate v.1.0.1 with the PlasmidFinder (62) database. Only plasmids with a similarity of more than 90% and a coverage over 95% were identified. BacAnt (63) was used to detect integrons and transposons in the genomes. Only integrons or transposons with a similarity of more than 60% and a coverage greater than 60% will be identified. The prophages were detected using the Phaster pipeline. The genomic data were split into two temporary databases based on the number of contigs, one dataset containing single contig files and the other containing multiple contig files. The two databases were imported into the Phaster pipeline separately with default parameters.

Determination of the MGE carried ARG and horizontal ARG transfer frequency

We have devised a pipeline to discern the coexistence of MGEs and ARGs. For plasmids and prophages, only ARGs situated within MGE regions are deemed MGE-carried. Regarding transposons and integrons, the search region was expanded to 5 kilobases upstream and downstream of ARGs, accounting for potential splicing errors. In this study, HGT events involving ARGs were defined as instances where ARGs exhibited perfect identity (100% coverage and 100% identity) and were located on MGEs across different strains. In a previous study

(64), horizontal transfer of ARGs was identified based on gene regions with 100% coverage and over 99% identity. We believe that these stricter criteria in our pipeline more accurately reflect the transfer of ARGs within the *S.* Gallinarum population. HGT frequency was utilized to evaluate the extent of horizontal transfer of ARGs as follows:

$$HGT\ frequency = \frac{\text{Horizontal ARG transfer Count}}{\text{Total dissemination count}}$$

The pipeline developed in this study accepts Resfinder or Resistance Gene Identifier (RGI) results as input. Specific code and examples are uploaded to: https://github.com/tjiaa/Cal_HGT_Frequency/tree/main.

Genomic data analysis

The serovars of all WGS genome data were confirmed through SISTR (65) v.1.1 and Seqsero2 (66). Multilocus Sequence Typing was carried out using MLST v.2.22 with the senterica_achtman_2 scheme. ARGs were detected by ResFinder (67). Both similarity and coverage were set to a minimum value of 90. The invasiveness index was calculated using methods previously reported (32). Specifically, *Salmonella*'s ability to cause intestinal or extraintestinal infections in hosts is related to the degree of genome degradation. We evaluated the potential for extraintestinal infection by 45 newly isolated *S*. Gallinarum strains (L2b and L3b) using a model that quantitatively assesses genome degradation. We analyzed each sample using the 196 top predictor genes for measuring the invasiveness of *S*. Gallinarum, employing a machine-learning approach that utilizes a random forest classifier and delta-bitscore functional variant-calling. This method evaluated the invasiveness of *S*. Gallinarum towards the host, and the distribution of invasiveness index values for each region was statistically

tested using unpaired *t*-test. The code used for calculating the invasiveness index is available at https://github.com/Gardner-BinfLab/invasive_salmonella.

ARGs vertical evolution control

In this study, HGTphyloDetect pipeline (68) was used to control for vertical evolution in the ARG sequences mentioned. We extracted base sequences for the eight ARGs shown in Figure 6b with an HGT frequency greater than zero (*bla*$_{\text{TEM-1B}}$, *sul1*, *dfrA17*, *aadA5*, *sul2*, *aph(3'')-Ib*, *tet(A)*, *aph(6)-Id*). For *bla*$_{\text{TEM-1B}}$, *sul1*, *dfrA17*, *aadA5*, and *sul2*, the HGT frequency reached 100% across different isolates, indicating that these ARG sequences have a unique ancestral sequence type. In contrast, due to the ResFinder settings requiring both similarity and coverage to meet a minimum value of 90%, the base sequences for *aph(3'')-Ib*, *tet(A)*, and *aph(6)-Id* are not unique. Consequently, we applied the HGTphyloDetect pipeline individually to each sequence type of ARGs to verify their association with HGT events. Specifically, among 436 bvSP isolates collected in China, we identified two sequence types of *aph(3'')-Ib*, four sequence types of *tet(A)*, and three sequence types of *aph(6)-Id*.

Subsequently, to identify potential ARGs horizontally acquired from evolutionarily distant organisms, we queried the translated amino acid sequences of each ARG against the National Center for Biotechnology Information (NCBI) non-redundant protein database. We then evaluated whether these sequences were products of HGT by calculating Alien Index (AI) scores and out_perc values. The calculation of Alien AI score is as follows:

$$AI\ score = \text{In}\ (bbhG + 1 \cdot 10^{-200})\ -\ \text{In}\ (bbhO + 1 \cdot 10^{-200})$$

In this study, bbhG and bbhO represent the E-values of the best blast hit in ingroup and outgroup lineages, respectively. The outgroup lineage is defined as all species outside of the kingdom, while the ingroup lineage encompasses species within the kingdom but outside of the subphylum. Regarding the calculation method for out_perc:

$$out_pect = n_{outside\ kingdom} / n_{total\ hits}$$

Finally, according to the definition provided by the HGTphyloDetect pipeline, ARGs with AI score ≥ 45 and out_perc ≥ 90% are presumed to be potential candidates for HGT from evolutionarily distant species.

Data Availability

For the newly isolated 45 strains of *Salmonella* Gallinarum, genome data have been deposited in NCBI Sequence Read Archive (SRA) database. The “SRA Accession” for each strain are listed in Supplementary Table 1. Additionally, the genome data for the 540 publicly available genomes (Supplementary Table 2) have been uploaded to Figureshare and can be accessed at: https://figshare.com/articles/journal_contribution/Genomic_data/26028592.

Code availability

The open-source software used in this study includes:

BacAnt (https://github.com/xthua/bacant),

Abricate (https://github.com/tseemann/abricate),

Snippy (https://github.com/tseemann/snippy),

SISTR (https://github.com/phac-nml/sistr_cmd),

MLST (https://cge.food.dtu.dk/services/MLST/)

SeqSero2 (https://github.com/denglab/SeqSero2),

IQtree (https://github.com/iqtree/iqtree2).

BEAST (https://www.beast2.org)

SNP-dists (https://github.com/tseemann/snp-dists)

Fast BAPS (https://github.com/gtonkinhill/fastbaps)

R (https://www.r-project.org)

Phaster (http://phaster.ca)

KmerFinder (https://bitbucket.org/genomicepidemiology/kmerfinder)

Treetime (https://github.com/neherlab/treetime)

Author contributions

M.Y., C.J. designed the study; finalized the manuscript;

C.J. collected isolates and clinical data, integrated the data, performed metadata and genomic analysis, prepared tables and figures; and wrote the draft manuscript;

C.H. performed metadata and genomic analysis; interpreted the data; finalized the manuscript;

X.Z., X.K., Q.C., Y.H. and Z.W. contributed to the data analysis;

C.H., M.Y. prepared tables and figures;

M.Y., C.H., A.S., Y.L., F.H., and C.J. finalized the manuscript;

M.Y. managed the project;

All the authors contributed to the article and approved the submitted version.

Declaration of Interests

None.

Acknowledgements

This work was supported by the National Program on the Key Research Project of China (2022YFC2604201), the Zhejiang Provincial Natural Science Foundation of China (LZ24C180002; LR19C180001), the Hainan Provincial Joint Project of Sanya Yazhou Bay Science and Technology City (2021JJLH0083), the Zhejiang Provincial Key R&D Program of China (2023C03045, 2022C02024) and the Open Project Program of the Jiangsu Key Laboratory of Zoonosis (R1902). We also thank Dr. Peide Li for providing the valuable resource for this investigation.

Reference

1. Li Y, Ed-Dra A, Tang B, Kang X, Müller A, Kehrenberg C, Jia C, Pan H, Yang H, Yue M. 2022. Higher tolerance of predominant Salmonella serovars circulating in the antibiotic-free feed farms to environmental stresses. Journal of Hazardous Materials 438:129476.

2. Hou J, Long X, Wang X, Li L, Mao D, Luo Y, Ren H. 2023. Global trend of antimicrobial resistance in common bacterial pathogens in response to antibiotic consumption. Journal of Hazardous Materials 442:130042.

3. Lee K, Raguideau S, Sirén K, Asnicar F, Cumbo F, Hildebrand F, Segata N, Cha C-J, Quince C. 2023. Population-level impacts of antibiotic usage on the human gut microbiome. Nat Commun 14:1191.

4. Rappuoli R, Bloom DE, Black S. 2017. Deploy vaccines to fight superbugs. Nature 552:165–167.

5. Larsson DGJ, Flach C-F. 2022. Antibiotic resistance in the environment. Nat Rev Microbiol 20:257–269.

6. Tóth AG, Judge MF, Nagy SÁ, Papp M, Solymosi N. 2023. A survey on antimicrobial resistance genes of frequently used probiotic bacteria, 1901 to 2022. Eurosurveillance 28.

7. Jia C, Wang Z, Huang C, Teng L, Zhou H, An H, Liao S, Liu Y, Huang L, Tang B, Yue M. 2023. Mobilome-driven partitions of the resistome in *Salmonella*. mSystems 8:e00883-23.

8. Carr VR, Witherden EA, Lee S, Shoaie S, Mullany P, Proctor GB, Gomez-Cabrero D, Moyes DL. 2020. Abundance and diversity of resistomes differ between healthy human oral cavities and gut. Nat Commun 11:693.

9. Wang Z, Huang C, Liu Y, Chen J, Yin R, Jia C, Kang X, Zhou X, Liao S, Jin X, Feng M, Jiang Z, Song Y, Zhou H, Yao Y, Teng L, Wang B, Li Y, Yue M.

2024. Salmonellosis outbreak archive in China: data collection and assembly. Sci Data 11:244.

10. Jia C, Cao Q, Wang Z, Van Den Dool A, Yue M. 2024. Climate change affects the spread of typhoid pathogens. Microbial Biotechnology 17:e14417.

11. Petersen E, Petrosillo N, Koopmans M, Beeching N, Di Caro A, Gkrania-Klotsas E, Kantele A, Kohlmann R, Koopmans M, Lim P-L, Markotic A, López-Vélez R, Poirel L, Rossen JWA, Stienstra Y, Storgaard M. 2018. Emerging infections—an increasingly important topic: review by the Emerging Infections Task Force. Clinical Microbiology and Infection 24:369–375.

12. Wang Z, Zhou H, Liu Y, Huang C, Chen J, Siddique A, Yin R, Jia C, Li Y, Zhao G, Yue M. 2024. Nationwide trends and features of human salmonellosis outbreaks in China. Emerging Microbes & Infections 13:2372364.

13. Ke Y, Teng L, Zhu Z, Lu W, Liu W, Zhou H, Yu Q, Ye L, Zhu P, Zhao G, Yue M. 2024. Genomic investigation and nationwide tracking of pediatric invasive nontyphoidal *Salmonella* in China. mLife 3:156–160.

14. Baquero F, Martínez JL, F. Lanza V, Rodríguez-Beltrán J, Galán JC, San Millán A, Cantón R, Coque TM. 2021. Evolutionary Pathways and Trajectories in Antibiotic Resistance. Clin Microbiol Rev 34:e00050-19.

15. Didelot X, Bowden R, Wilson DJ, Peto TEA, Crook DW. 2012. Transforming clinical microbiology with bacterial genome sequencing. Nat Rev Genet 13:601–612.

16. Chen J, Huang L, An H, Wang Z, Kang X, Yin R, Jia C, Jin X, Yue M. 2024. One Health approach probes zoonotic non-typhoidal *Salmonella* infections in China: A systematic review and meta-analysis. J Glob Health 14:04256.

17. Gossner CM, Le Hello S, De Jong B, Rolfhamre P, Faensen D, Weill F-X, Johan Giesecke. 2016. Around the World in 1,475 *Salmonella* Geo-serotypes. Emerg Infect Dis 22:1298–1302.

18. Kang X, Jin C, Gu P, Wang S, Gao Z, Dai C, Zhou X, Siddique A, Zhou H, Huang L, Li Y, Yue M. 2024. A dynamic platform for global pullorum disease and fowl typhoid. Animal Diseases 4:39.

19. Kang X, Zhou X, Tang Y, Jiang Z, Chen J, Mohsin M, Yue M. 2022. Characterization of Two-Component System CitB Family in Salmonella Pullorum. IJMS 23:10201.

20. Zhou X, Kang X, Zhou K, Yue M. 2022. A global dataset for prevalence of Salmonella Gallinarum between 1945 and 2021. Sci Data 9:495.

21. Zhou X, Kang X, Chen J, Song Y, Jia C, Teng L, Tang Y, Jiang Z, Peng X, Tao X, Xu Y, Huang L, Xu X, Xu Y, Zhang T, Yu S, Gong J, Wang S, Liu Y, Zhu G, Kehrenberg C, Weill F-X, Barrow P, Li Y, Zhao G, Yue M. 2023. Genome degradation promotes *Salmonella* pathoadaptation by remodeling fimbriae-mediated proinflammatory response. National Science Review 10:nwad228.

22. De Carli S, Gräf T, Kipper D, Lehmann FKM, Zanetti N, Siqueira FM, Cibulski S, Fonseca ASK, Ikuta N, Lunge VR. 2017. Molecular and phylogenetic analyses of Salmonella Gallinarum trace the origin and diversification of recent outbreaks of fowl typhoid in poultry farms. Veterinary Microbiology 212:80–86.

23. Barrow PA, Neto OCF. 2011. Pullorum disease and fowl typhoid—new thoughts on old diseases: a review. Avian Pathology 40:1–13.

24. Nhung NT, Chansiripornchai N, Carrique-Mas JJ. 2017. Antimicrobial Resistance in Bacterial Poultry Pathogens: A Review. Front Vet Sci 4:126.

25. Penha Filho RAC, Ferreira JC, Kanashiro AMI, Darini AL da C, Berchieri Junior A. 2016. Antimicrobial susceptibility of Salmonella Gallinarum and

Salmonella Pullorum isolated from ill poultry in Brazil. Ciência Rural 46:513–518.

26. Jia C, Huang L, Zhou H, Cao Q, Wang Z, He F, Li Y, Yue M. 2024. A global genome dataset for Salmonella Gallinarum recovered between 1920 and 2024. Sci Data 11:1094.

27. Huang L, Zhou H, Chen J, Jia C, Siddique A, Wu B, Wang H, Tang B, He F, Zhao G, Yue M. 2024. Impact of COVID-19-related nonpharmaceutical interventions on diarrheal diseases and zoonotic Salmonella. hLife S294992832400021X.

28. Kisiela D, Kuczkowski M, Kiczak L, Wieliczko A, Ugorski M. 2005. Differentiation of *Salmonella* Gallinarum biovar Gallinarum from *Salmonella* Gallinarum biovar Pullorum by PCR-RFLP of the *fimH* gene. Journal of Veterinary Medicine, Series B 52:214–218.

29. Burnham GP. 1855. The history of the hen fever: a humorous record. James French.

30. Cuypers WL, Meysman P, Weill F-X, Hendriksen RS, Beyene G, Wain J, Nair S, Chattaway MA, Perez-Sepulveda BM, Ceyssens P-J, De Block T, Lee WWY, Pardos De La Gandara M, Kornschober C, Moran-Gilad J, Veldman KT, Cormican M, Torpdahl M, Fields PI, Černý T, Hardy L, Tack

B, Mellor KC, Thomson N, Dougan G, Deborggraeve S, Jacobs J, Laukens K, Van Puyvelde S. 2023. A global genomic analysis of Salmonella Concord reveals lineages with high antimicrobial resistance in Ethiopia. Nat Commun 14:3517.

31. Pulford CV, Perez-Sepulveda BM, Canals R, Bevington JA, Bengtsson RJ, Wenner N, Rodwell EV, Kumwenda B, Zhu X, Bennett RJ, Stenhouse GE, Malaka De Silva P, Webster HJ, Bengoechea JA, Dumigan A, Tran-Dien A, Prakash R, Banda HC, Alufandika L, Mautanga MP, Bowers-Barnard A, Beliavskaia AY, Predeus AV, Rowe WPM, Darby AC, Hall N, Weill F-X, Gordon MA, Feasey NA, Baker KS, Hinton JCD. 2020. Stepwise evolution of Salmonella Typhimurium ST313 causing bloodstream infection in Africa. Nat Microbiol 6:327–338.

32. Van Puyvelde S, Pickard D, Vandelannoote K, Heinz E, Barbé B, De Block T, Clare S, Coomber EL, Harcourt K, Sridhar S, Lees EA, Wheeler NE, Klemm EJ, Kuijpers L, Mbuyi Kalonji L, Phoba M-F, Falay D, Ngbonda D, Lunguya O, Jacobs J, Dougan G, Deborggraeve S. 2019. An African Salmonella Typhimurium ST313 sublineage with extensive drug-resistance and signatures of host adaptation. Nat Commun 10:4280.

33. Worboys M. 2000. Spreading germs: disease theories and medical practice in Britain, 1865-1900. Cambridge University Press.

34. Porter R, Crosby AW. 1998. The Greatest Benefit to Mankind: A Medical History of Humanity from Antiquity to the Present. Nature 391:241–241.

35. Helekal D, Keeling M, Grad YH, Didelot X. 2023. Estimating the fitness cost and benefit of antimicrobial resistance from pathogen genomic data. J R Soc Interface 20:20230074.

36. Gong J, Xu M, Zhu C, Miao J, Liu X, Xu B, Zhang J, Yu Y, Jia X. 2013. Antimicrobial resistance, presence of integrons and biofilm formation of *Salmonella* Pullorum isolates from eastern China (1962–2010). Avian Pathology 42:290–294.

37. Li Y, Teng L, Xu X, Li X, Peng X, Zhou X, Du J, Tang Y, Jiang Z, Wang Z, Jia C, Müller A, Kehrenberg C, Wang H, Wu B, Weill F, Yue M. 2022. A nontyphoidal *Salmonella* serovar domestication accompanying enhanced niche adaptation. EMBO Mol Med 14:e16366.

38. Teng L, Liao S, Zhou X, Jia C, Feng M, Pan H, Ma Z, Yue M. 2022. Prevalence and Genomic Investigation of Multidrug-Resistant Salmonella Isolates from Companion Animals in Hangzhou, China. Antibiotics 11:625.

39. Pan H, Jia C, Paudyal N, Li F, Mao J, Liu X, Dong C, Zhou K, Liao X, Gong J, Fang W, Li X, Kehrenberg C, Yue M. 2022. Comprehensive Assessment

of Subtyping Methods for Improved Surveillance of Foodborne Salmonella. Microbiol Spectr 10:e02479-22.

40. Kumar D, Pornsukarom S, Thakur S. 2019. Antibiotic usage in poultry production and antimicrobial-resistant Salmonella in poultry. Food safety in poultry meat production 47–66.

41. Jin C, Jia C, Hu W, Xu H, Shen Y, Yue M. 2024. Predicting antimicrobial resistance in E. coli with discriminative position fused deep learning classifier. Computational and Structural Biotechnology Journal 23:559–565.

42. Elbediwi M, Tang Y, Shi D, Ramadan H, Xu Y, Xu S, Li Y, Yue M. 2021. Genomic Investigation of Antimicrobial-Resistant Salmonella enterica Isolates From Dead Chick Embryos in China. Front Microbiol 12:684400.

43. Li Y, Kang X, Ed-Dra A, Zhou X, Jia C, Müller A, Liu Y, Kehrenberg C, Yue M. 2022. Genome-Based Assessment of Antimicrobial Resistance and Virulence Potential of Isolates of Non-Pullorum/Gallinarum Salmonella Serovars Recovered from Dead Poultry in China. Microbiol Spectr 10:e00965-22.

44. Xu Y, Zhou X, Jiang Z, Qi Y, Ed-dra A, Yue M. 2020. Epidemiological Investigation and Antimicrobial Resistance Profiles of Salmonella Isolated

From Breeder Chicken Hatcheries in Henan, China. Front Cell Infect Microbiol 10:497.

45. Jin X, Peng N, Cui A, Liu Y, Peng X, Huang L, Ed-Dra A, He F, Li Y, Yang S, Yue M. 2024. Sodium dodecyl sulfate-coated silver nanoparticles accelerate antimicrobial potentials by targeting amphiphilic membranes. mLife 3:551–564.

46. Golkar Z, Bagasra O, Pace DG. 2014. Bacteriophage therapy: a potential solution for the antibiotic resistance crisis. J Infect Dev Ctries 8:129–136.

47. Kang X, An H, Wang B, Huang L, Huang C, Huang Y, Wang Z, He F, Li Y, Yue M. 2024. Integrated OMICs approach reveals energy metabolism pathway is vital for *Salmonella* Pullorum survival within the egg white. mSphere 9:e00362-24.

48. Peng X, Ed-Dra A, Song Y, Elbediwi M, Nambiar RB, Zhou X, Yue M. 2022. Lacticaseibacillus rhamnosus alleviates intestinal inflammation and promotes microbiota-mediated protection against Salmonella fatal infections. Front Immunol 13:973224.

49. Siddique A, Wang Z, Zhou H, Huang L, Jia C, Wang B, Ed-Dra A, Teng L, Li Y, Yue M. 2024. The Evolution of Vaccines Development across

Salmonella Serovars among Animal Hosts: A Systematic Review. Vaccines 12:1067.

50. Jiang Z, Kang X, Song Y, Zhou X, Yue M. 2023. Identification and Evaluation of Novel Antigen Candidates against Salmonella Pullorum Infection Using Reverse Vaccinology. Vaccines 11:865.

51. Bankevich A, Nurk S, Antipov D, Gurevich AA, Dvorkin M, Kulikov AS, Lesin VM, Nikolenko SI, Pham S, Prjibelski AD, Pyshkin AV, Sirotkin AV, Vyahhi N, Tesler G, Alekseyev MA, Pevzner PA. 2012. SPAdes: A New Genome Assembly Algorithm and Its Applications to Single-Cell Sequencing. Journal of Computational Biology 19:455–477.

52. Ellington MJ, Ekelund O, Aarestrup FM, Canton R, Doumith M, Giske C, Grundman H, Hasman H, Holden MTG, Hopkins KL, Iredell J, Kahlmeter G, Köser CU, MacGowan A, Mevius D, Mulvey M, Naas T, Peto T, Rolain J-M, Samuelsen Ø, Woodford N. 2017. The role of whole genome sequencing in antimicrobial susceptibility testing of bacteria: report from the EUCAST Subcommittee. Clinical Microbiology and Infection 23:2–22.

53. Hasman H, Saputra D, Sicheritz-Ponten T, Lund O, Svendsen CA, Frimodt-Møller N, Aarestrup FM. 2014. Rapid Whole-Genome Sequencing for Detection and Characterization of Microorganisms Directly from Clinical Samples. J Clin Microbiol 52:139–146.

54. Nguyen L-T, Schmidt HA, Von Haeseler A, Minh BQ. 2015. IQ-TREE: A Fast and Effective Stochastic Algorithm for Estimating Maximum-Likelihood Phylogenies. Molecular Biology and Evolution 32:268–274.

55. Letunic I, Bork P. 2021. Interactive Tree Of Life (iTOL) v5: an online tool for phylogenetic tree display and annotation. Nucleic Acids Research 49:W293–W296.

56. Cheng L, Connor TR, Siren J, Aanensen DM, Corander J. 2013. Hierarchical and Spatially Explicit Clustering of DNA Sequences with BAPS Software. Molecular Biology and Evolution 30:1224–1228.

57. Croucher NJ, Page AJ, Connor TR, Delaney AJ, Keane JA, Bentley SD, Parkhill J, Harris SR. 2015. Rapid phylogenetic analysis of large samples of recombinant bacterial whole genome sequences using Gubbins. Nucleic Acids Research 43:e15–e15.

58. Sagulenko P, Puller V, Neher RA. 2018. TreeTime: Maximum-likelihood phylodynamic analysis. Virus Evolution 4.

59. Bouckaert R, Vaughan TG, Barido-Sottani J, Duchêne S, Fourment M, Gavryushkina A, Heled J, Jones G, Kühnert D, De Maio N, Matschiner M, Mendes FK, Müller NF, Ogilvie HA, Du Plessis L, Popinga A, Rambaut A,

Rasmussen D, Siveroni I, Suchard MA, Wu C-H, Xie D, Zhang C, Stadler T, Drummond AJ. 2019. BEAST 2.5: An advanced software platform for Bayesian evolutionary analysis. PLoS Comput Biol 15:e1006650.

60. Pightling AW, Rand H, Pettengill J. 2022. Using Evolutionary Analyses to Refine Whole-Genome Sequence Match Criteria. Front Microbiol 13:797997.

61. Feng Y, Pan H, Zheng B, Li F, Teng L, Jiang Z, Feng M, Zhou X, Peng X, Xu X, Wang H, Wu B, Xiao Y, Baker S, Zhao G, Yue M. 2023. An integrated nationwide genomics study reveals transmission modes of typhoid fever in China. mBio 14:e01333-23.

62. Carattoli A, Zankari E, García-Fernández A, Voldby Larsen M, Lund O, Villa L, Møller Aarestrup F, Hasman H. 2014. *In Silico* Detection and Typing of Plasmids using PlasmidFinder and Plasmid Multilocus Sequence Typing. Antimicrob Agents Chemother 58:3895–3903.

63. Hua X, Liang Q, Deng M, He J, Wang M, Hong W, Wu J, Lu B, Leptihn S, Yu Y, Chen H. 2021. BacAnt: A Combination Annotation Server for Bacterial DNA Sequences to Identify Antibiotic Resistance Genes, Integrons, and Transposable Elements. Front Microbiol 12:649969.

64. Wang X, Zhang H, Yu S, Li D, Gillings MR, Ren H, Mao D, Guo J, Luo Y. 2024. Inter-plasmid transfer of antibiotic resistance genes accelerates antibiotic resistance in bacterial pathogens. The ISME Journal 18:wrad032.

65. Yoshida CE, Kruczkiewicz P, Laing CR, Lingohr EJ, Gannon VPJ, Nash JHE, Taboada EN. 2016. The Salmonella In Silico Typing Resource (SISTR): An Open Web-Accessible Tool for Rapidly Typing and Subtyping Draft Salmonella Genome Assemblies. PLoS ONE 11:e0147101.

66. Zhang S, Den Bakker HC, Li S, Chen J, Dinsmore BA, Lane C, Lauer AC, Fields PI, Deng X. 2019. SeqSero2: Rapid and Improved *Salmonella* Serotype Determination Using Whole-Genome Sequencing Data. Appl Environ Microbiol 85:e01746-19.

67. Zankari E, Hasman H, Cosentino S, Vestergaard M, Rasmussen S, Lund O, Aarestrup FM, Larsen MV. 2012. Identification of acquired antimicrobial resistance genes. Journal of Antimicrobial Chemotherapy 67:2640–2644.

68. Yuan L, Lu H, Li F, Nielsen J, Kerkhoven EJ. 2023. HGTphyloDetect: facilitating the identification and phylogenetic analysis of horizontal gene transfer. Briefings in Bioinformatics 24:bbad035.

Figure Legends

Figure 1. Genetic diversity of *S*. Gallinarum biovar Pullorum (bvSP) by geography and time. Different colours were used to represent the various lineages of bvSP: fuchsia for L1, orange for L2a, pink for L2b, red for L3b, and green for L3c. (a) The bvSP in the dataset is classified into five continents based on their isolation regions. The bar graph illustrates the distribution of lineage-specific bvSP across continents, depicted as percentages. The total sample size for each bar is indicated at the top. (b) Geographic distribution of bvSP isolated from China. Doughnut charts in the map show the proportion of lineage types of bvSP collected in the corresponding region, with the total number of isolates in the center. (c) The bar graph shows the distribution of bvSP isolated in China by lineage per decade. The total sample size for each bar is also indicated on the right side.

Figure 2. Phylogenetic tree of *S.* Gallinarum L2b and L3b based on a spatiotemporal Bayesian framework. The phylogenetic tree on the left was constructed using a reference-mapped multiple core-genome SNPs sequence alignment, with recombination regions detected and removed by Gubbins. The spatiotemporal Bayesian framework was configured with the "GTR" substitution model, 4 Gamma Category Count, "Relaxed Clock Log Normal" model, "Coalescent Bayesian Skyline" tree prior model, and a Markov Chain Monte Carlo (MCMC) chain length of 100,000,000, with sampling every 10,000 iterations. Convergence was assessed using Tracer, ensuring all parameter effective sampling sizes (ESS) exceeded 200. Evolutionary time is represented by the length of the branches. The heatmap on the right displays, respectively, the sequence type (ST), region of isolation, and the number (Num.) of antimicrobial resistance genes (ARGs) carried by the corresponding *Salmonella* Gallinarum.

Figure 3. Genomic characteristics of 45 newly isolated *S*. Gallinarum biovar Pullorum (bvSP) strains from Taishun and Yueqing, Zhejiang Province, China. (a) The phylogenetic tree, constructed using cgSNPs, categorizes the 45 bvSP strains into two distinct lineages (L3b and L2b). On the left side of the heatmap, information on isolation regions, sequence types (ST), and sampling times are displayed, with various colors indicating different categories as specified on the left. The right section of the heatmap presents a detailed matrix showing plasmids, ARGs, and cgSNP distances. The presence of a plasmid or ARG in an isolate is denoted by gray shading, while absence is indicated by white. cgSNPs below two were used as the threshold, with red circles signifying a higher probability of transmission between isolate pairs. (b) The average cgSNP distance between isolates from Taishun and Yueqing. E404 led to an increase in the mean cgSNP distance of bvSP from Taishun. (c) Invasiveness index of bvSP in Taishun and Yueqing. The results show a higher invasiveness index for bvSP isolated from Taishun, indicating that bvSP isolated from Taishun might have greater invasive capabilities among vulnerable hens.

Figure 4. The ARGs carried by *S.* Gallinarum. (a) The phylogenetic tree was constructed using cgSNPs, revealing three *S.* Gallinarum biovars: *S*. Gallinarum biovar Pullorum (bvSP), *S*. Gallinarum biovar Duisburg (bvSD), and *S*. Gallinarum biovar Gallinarum (bvSG). Additionally, *Salmonella serovar* Enteritidis (SE.) is represented by a gray line. Further, bvSP can be subdivided into five lineages: fuchsia (L1), orange (L2a), pink (L2b), red (L3b), and green (L3c). The heatmap on the right indicates the resistome carried by the corresponding *Salmonella*. (b) The dominant resistome types in different regions of China. The y-axis represents the percentage of each dominant

resistome. The total sample size for each bar is indicated at the top. (c) The average number of resistome carried by bvSP is from different regions of China.

Figure 5. The primary source of resistome is carried by distinct mobilome. Different font colours denote various mobilome types. Specifically, orange signifies Integrons, red denotes transposons, blue represents plasmids, and green indicates prophages. A black font is utilized to distinguish the categories of resistome. The connecting line between the resistome and the mobilome represents the potential carrying relationship. (a) The mobilome-carried ARGs among *S*. Gallinarum biovar Pullorum (bvSP). (b) The average number of ARGs carried by the four MGEs in bvSP. The unpaired *t*-test was used to compare the differences between isolates, with $P < 0.05$ considered statistically significant. (c-e) The mobilome-carried ARGs among bvSP isolated from the eastern, southern, and northern regions of China.

Figure 6. The HGT frequency of the resistome among *S*. Gallinarum biovar Pullorum (bvSP) isolated from China. (a) Workflow for identification of horizontally transferred ARGs in *Salmonella*. (b) The x-axis represents the resistome of bvSP, while the y-axis represents the corresponding levels of HGT frequency. (c) The HGT frequency level of specific ARGs carried by bvSP isolated from various regions of China. Deeper colours mean higher HGT frequency. (d) The frequency of horizontal retransmission of the resistome between different regions of China. A higher value indicates more frequent transfer events of resistome between two regions. The colors on the map represent the number of bvSP isolates in each region. Darker colors indicate a higher number of bvSP isolates in that area.

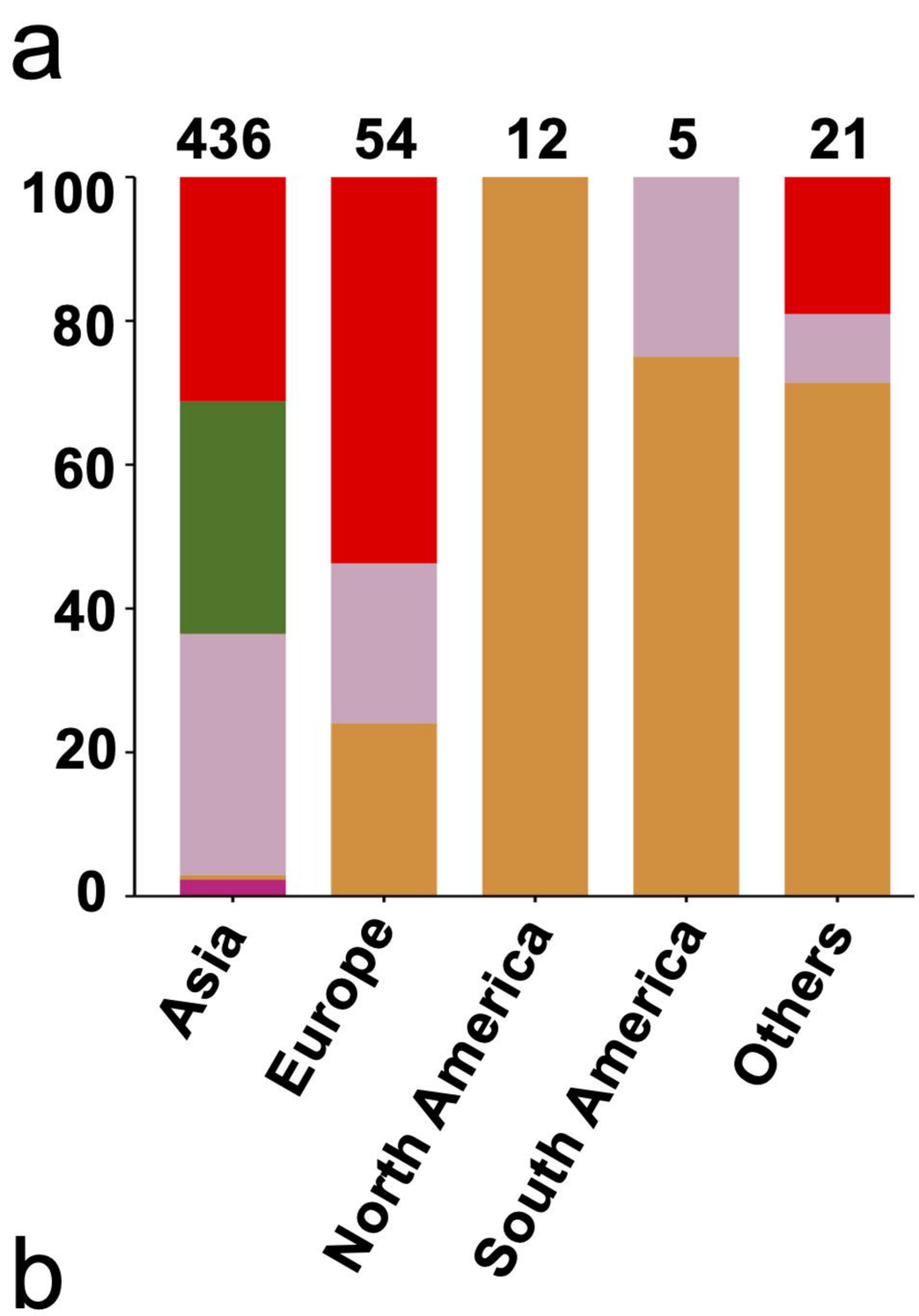
a
436
54
12
5
21
100
80
60
40
20
0
Asia
Europe
North America
South America
Others

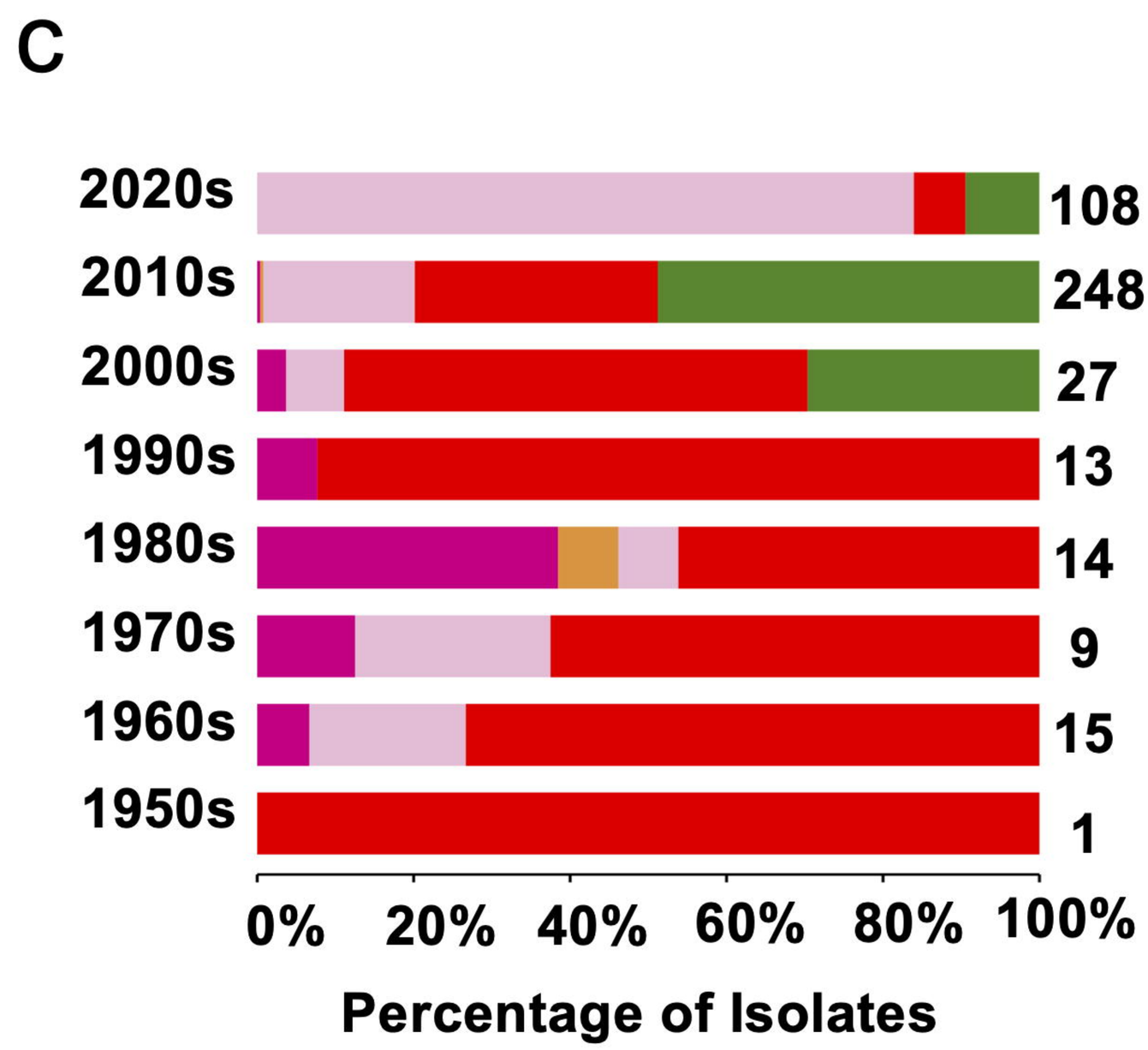
c
2020s
2010s
2000s
1990s
1980s
1970s
1960s
1950s
108
248
27
13
14
9
15
1
0%
20%
40%
60%
80%
100%
Percentage of Isolates

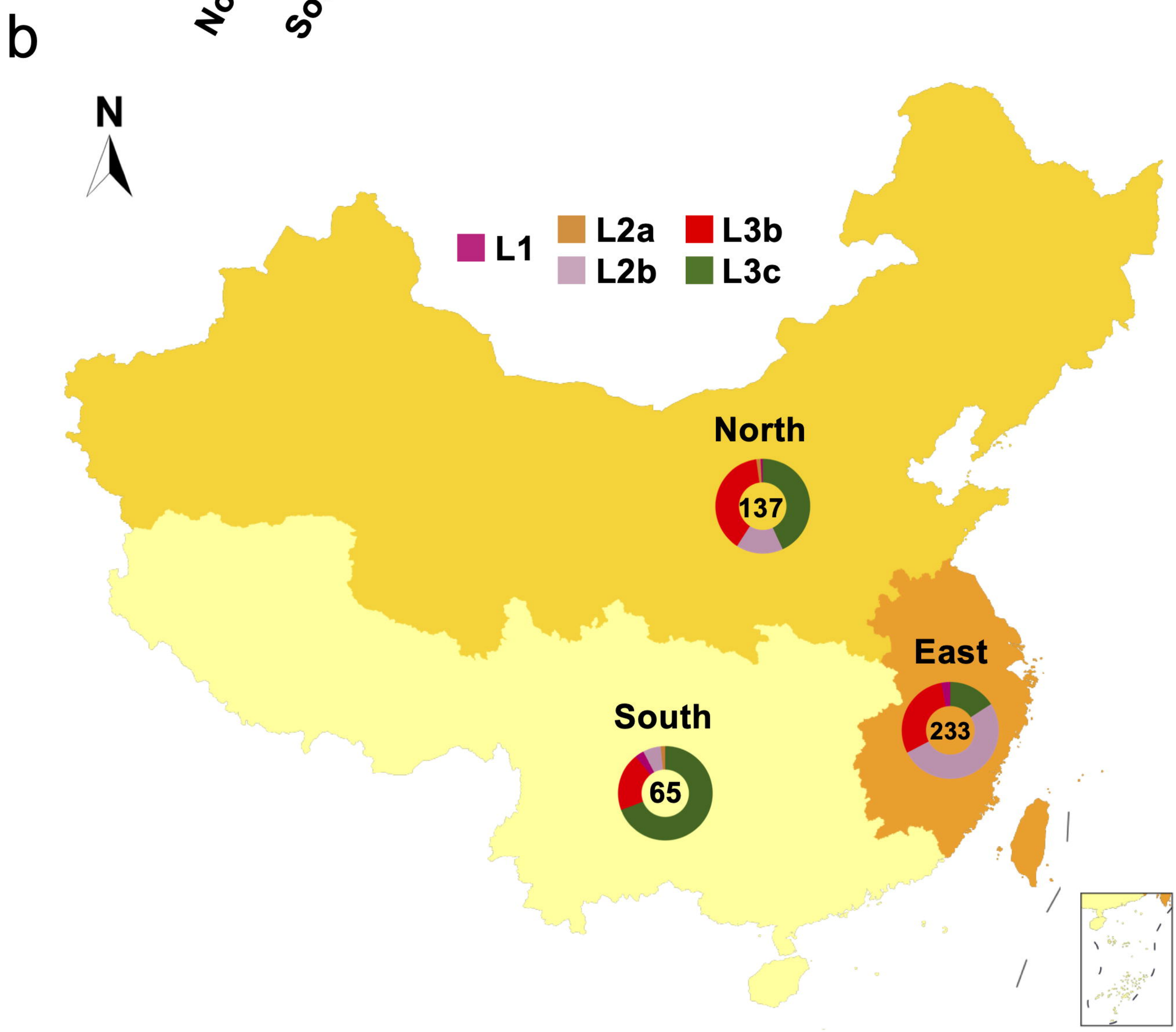
b
N
L1
L2a
L2b
L3b
L3c
North
137
East
233
South
65

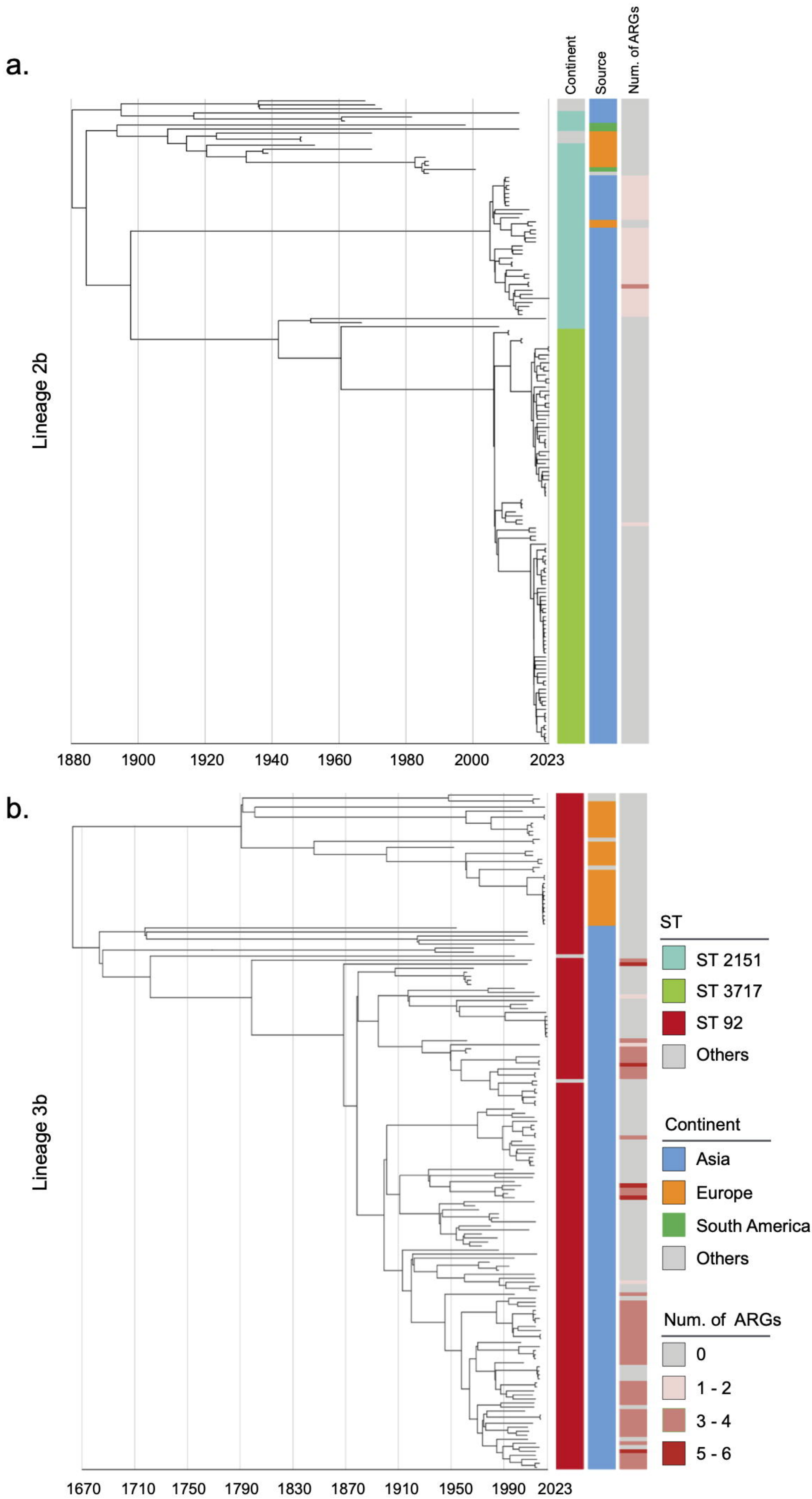
a.
Lineage 2b
Continent
Source
Num. of ARGs
1880
1900
1920
1940
1960
1980
2000
2023
b.
Lineage 3b
1670
1710
1750
1790
1830
1870
1910
1950
1990
2023
ST
ST 2151
ST 3717
ST 92
Others
Continent
Asia
Europe
South America
Others
Num. of ARGs
0
1 - 2
3 - 4
5 - 6

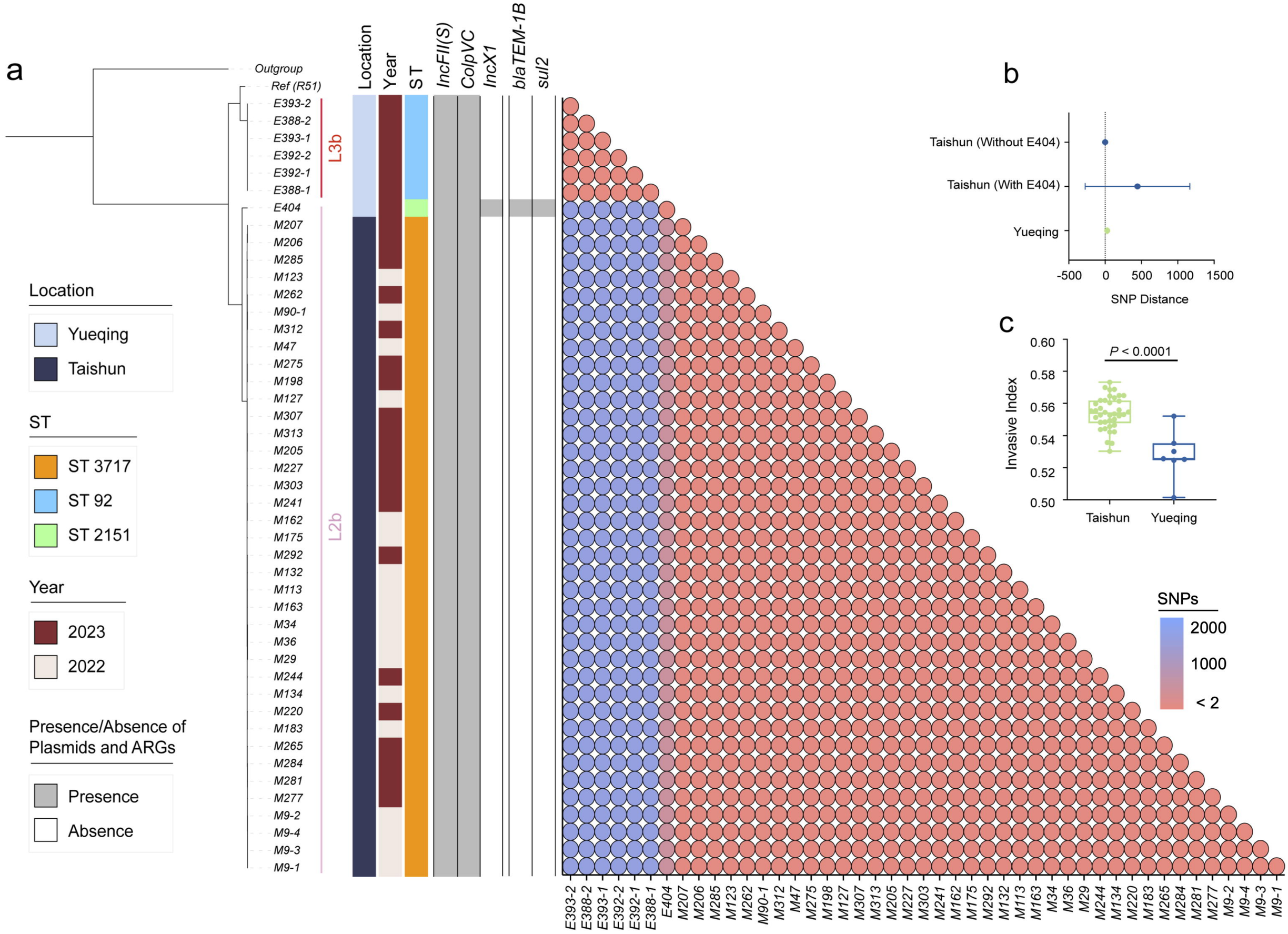
a
Outgroup
Ref (R51)
E393-2
E388-2
E393-1
E392-2
E392-1
E388-1
E404
M207
M206
M285
M123
M262
M90-1
M312
M47
M275
M198
M127
M307
M313
M205
M227
M303
M241
M162
M175
M292
M132
M113
M163
M34
M36
M29
M244
M134
M220
M183
M265
M284
M281
M277
M9-2
M9-4
M9-3
M9-1
L3b
L2b
Location
Year
ST
IncFII(S)
ColpVC
IncX1
blaTEM-1B
sul2
Location
Yueqing
Taishun
ST
ST 3717
ST 92
ST 2151
Year
2023
2022
Presence/Absence of Plasmids and ARGs
Presence
Absence
SNPs
2000
1000
< 2
b
Taishun (Without E404)
Taishun (With E404)
Yueqing
-500
0
500
1000
1500
SNP Distance
c
P < 0.0001
Invasive Index
0.60
0.58
0.56
0.54
0.52
0.50
Taishun
Yueqing

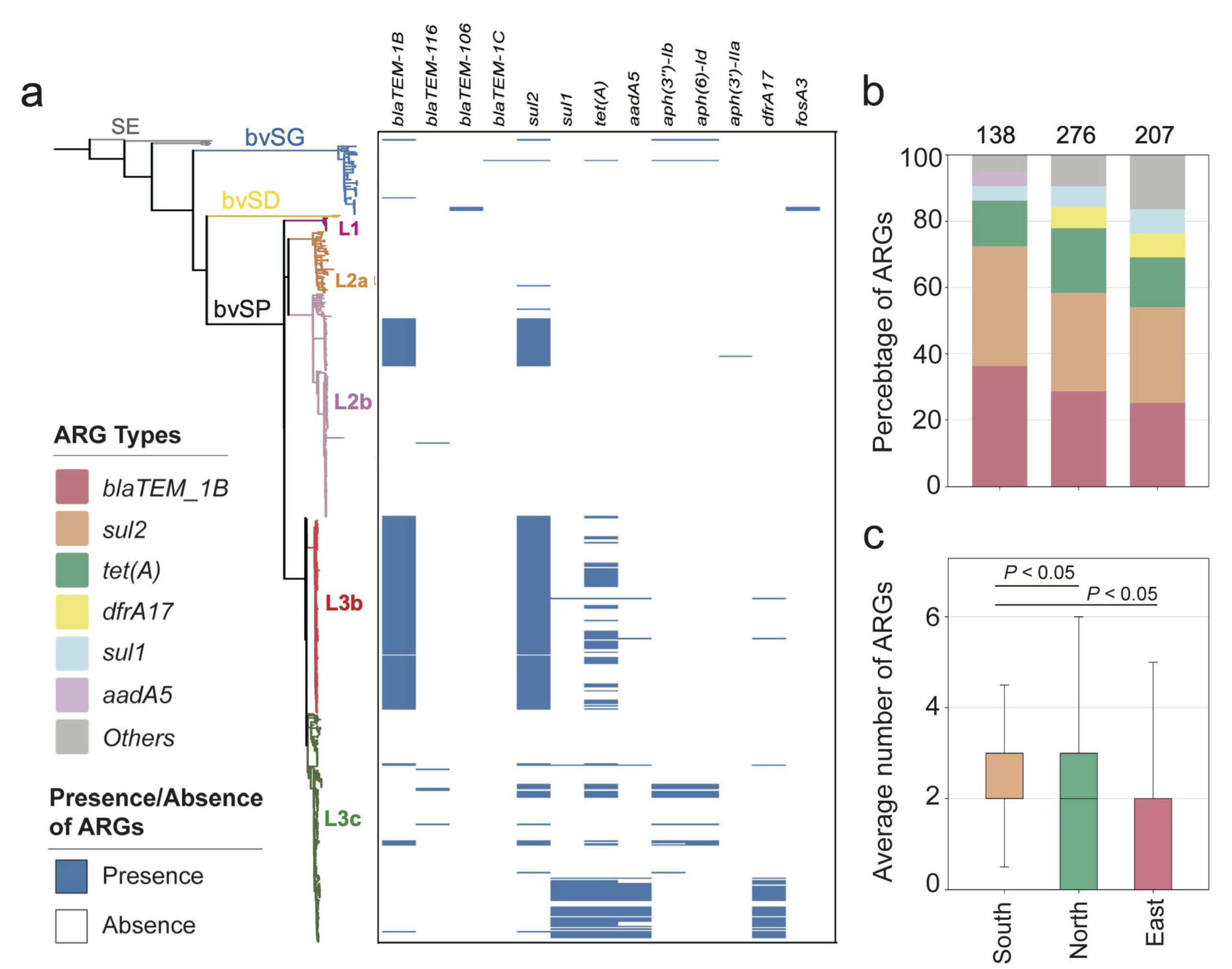
a
blaTEM-1B
blaTEM-116
blaTEM-106
blaTEM-1C
sul2
sul1
tet(A)
aadA5
aph(3'')-Ib
aph(6)-Id
aph(3')-IIa
dfrA17
fosA3
SE
bvSG
bvSD
bvSP
L1
L2a
L2b
L3b
L3c
ARG Types
blaTEM_1B
sul2
tet(A)
dfrA17
sul1
aadA5
Others
Presence/Absence of ARGs
Presence
Absence
b
138
276
207
Percebtage of ARGs
100
80
60
40
20
0
c
P < 0.05
P < 0.05
Average number of ARGs
6
4
2
0
South
North
East

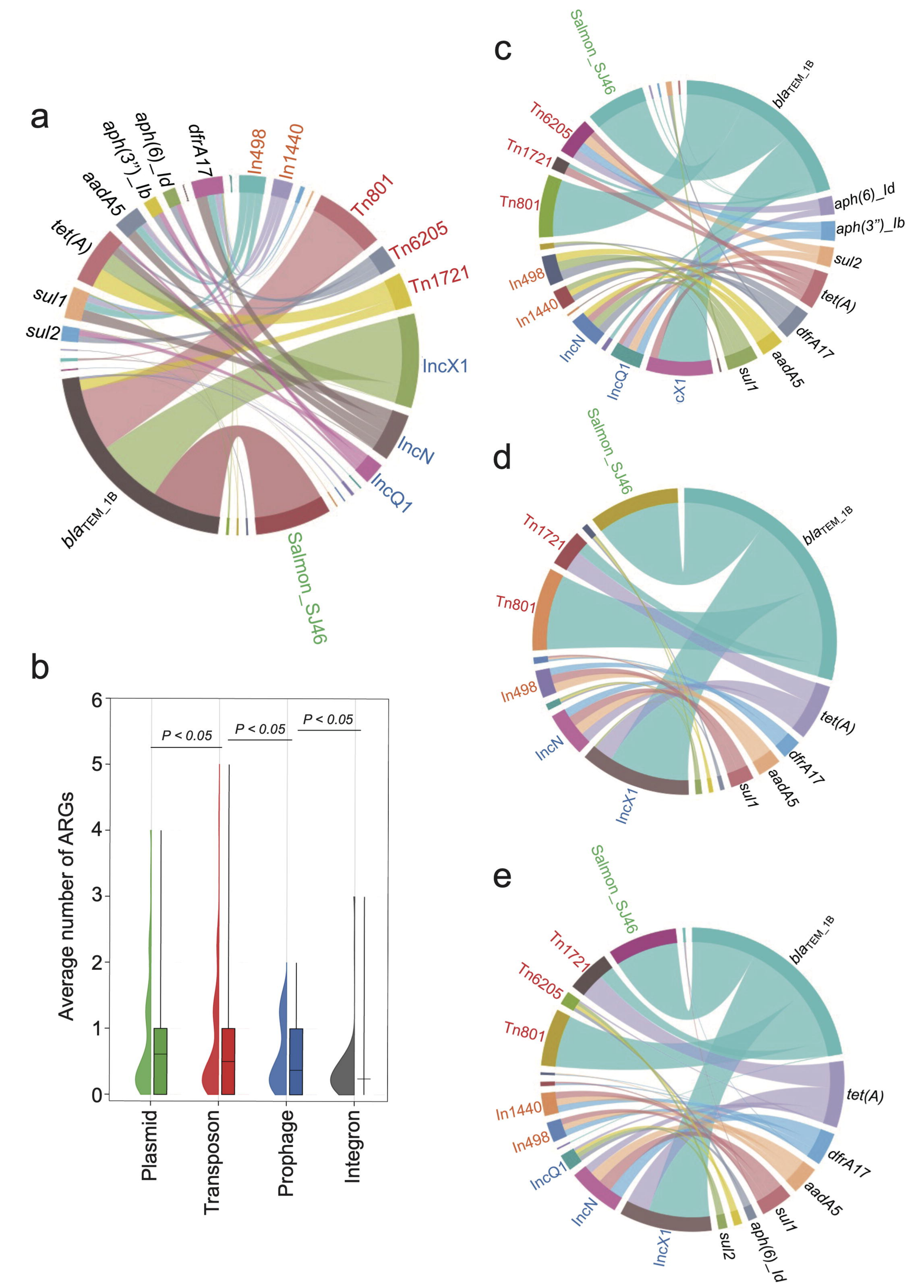
a
b
c
d
e
Average number of ARGs
P < 0.05
P < 0.05
P < 0.05
Plasmid
Transposon
Prophage
Integron
Salmon_SJ46
blaTEM_1B
Tn6205
Tn1721
Tn801
In498
In1440
IncN
IncQ1
IncX1
aph(6)_Id
aph(3")_Ib
sul2
tet(A)
dfrA17
aadA5
sul1

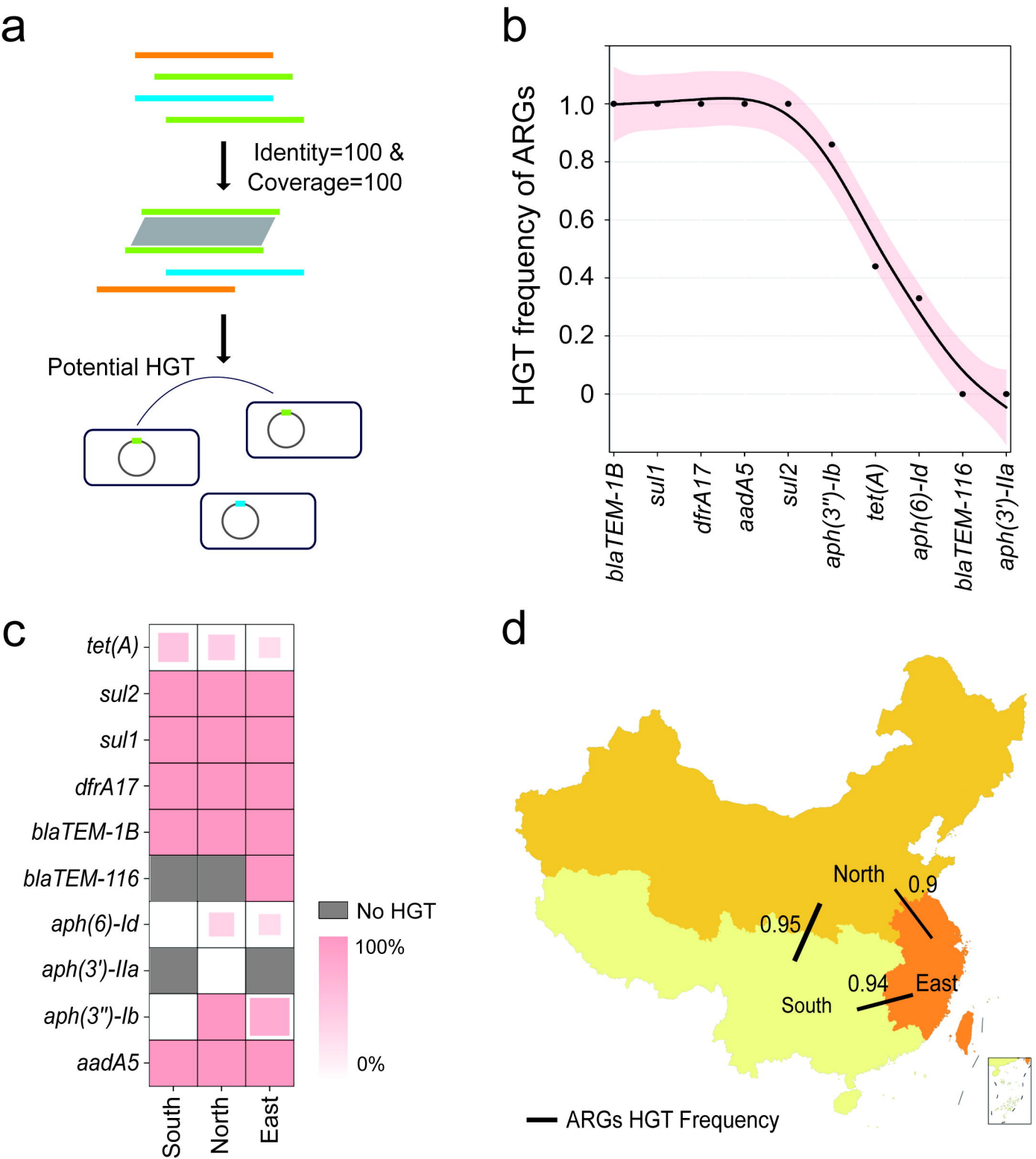
a
Identity=100 &
Coverage=100
Potential HGT
b
HGT frequency of ARGs
1.0
0.8
0.6
0.4
0.2
0
blaTEM-1B
sul1
dfrA17
aadA5
sul2
aph(3'')-Ib
tet(A)
aph(6)-Id
blaTEM-116
aph(3')-IIa
c
tet(A)
sul2
sul1
dfrA17
blaTEM-1B
blaTEM-116
aph(6)-Id
aph(3')-IIa
aph(3'')-Ib
aadA5
South
North
East
No HGT
100%
0%
d
North
0.9
0.95
0.94
East
South
ARGs HGT Frequency